Chemical Papers (2021) 75:2353–2369
https://doi.org/10.1007/s11696-020-01480-z

ORIGINAL PAPER

A highly effective green catalyst Ni/Cu bimetallic nanoparticles supported by dendritic ligand for chemoselective oxidation and reduction reaction

Md. Sayedul Islam[1] · **Md. Wahab Khan**[1]

Received: 25 May 2020 / Accepted: 18 December 2020 / Published online: 6 January 2021

Abstract

The highly active Ni/Cu bimetallic nanoparticles (NPs) of the different molar ratios of Ni and Cu (1:1, 1:3, 3:1) assisted by dendritic ligand 2,4,6-Tris (di-4-chlorobenzamido)-1,3-diazine were synthesized successfully confirmed by Scanning Electron Microscopy (SEM), Electron Diffraction X-ray (EDX), X-ray fluorescence spectroscopy (XRF), X-ray diffraction (XRD), and Transmission Electron Microscopy (TEM) analysis. These NPs were studied as a heterogeneous catalyst for the chemoselective oxidation of alcohol to the corresponding aldehyde at 30 min and chemoselective reduction of aromatic nitro substituents to the corresponding amino substituents at 20 min, while the Ni/Cu (3:1) NPs were found to be the most effective among other Ni/Cu (1:1) and Ni/Cu (1:3) NPs at room temperature under mild conditions. The Ni/Cu (3:1) NPs can be recycled for at least five successive runs with no perceptible decrease in catalytic activity.

Graphic abstract

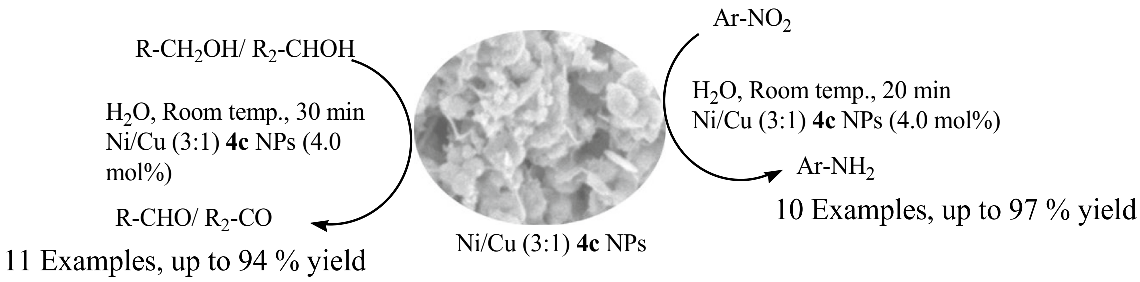

Keywords Dendritic · Nickel/copper bimetallic nanoparticles · Chemoselective · Oxidation · Reduction

Introduction

One of the significant chemical procedures for the synthesis of specific compounds is chemoselective oxidation of alcohols; it provides essential synthetics such as aldehydes, ketones, and carboxylic acids. Stoichiometric oxidation procedures applying homogeneous oxidants such as $KMnO_4$, $K_2Cr_2O_7$, and also the oxidation process catalyzed by the metal-complexes (Gong et al. 2016; Harada et al. 2010) have a long tradition of the oxidation reaction.

Also, in the chemical, petroleum, pharmaceutical, and agricultural industries, the chemoselective reduction of nitro compounds to the resulting amines is a crucial procedure

---

Supplementary Information The online version contains supplementary material available at https://doi.org/10.1007/s11696-020-01480-z.

✉ Md. Wahab Khan
mwkhan@chem.buet.ac.bd

Md. Sayedul Islam
sayedulbuet98@gmail.com

[1] Department of Chemistry, Faculty of Engineering, Bangladesh University of Engineering and Technology (BUET), Dhaka 1000, Bangladesh

(Hosseini-Sarvari and Razmi 2015); as a consequence of ordinarily using amines and their derivatives as intermediate for colorants of azo dyes, pigments in industrial chemicals and also in bioactive substances, medicinal, pesticides, insecticides, and fungicides (Yang et al. 2012a, b; Mondal and Purkait 2017; Harraz et al. 2012).

However, after forming the products, these general methods have noteworthy drawbacks resulting from the removal of salts, the separation of catalysts, and the refining of the yields. Therefore, it is essential to improve green catalytic methods under benign conditions to synthesis pure aldehydes, ketones, and amines through selective oxidation and reduction reactions.

Significantly, heterogeneous bimetallic NPs have revealed tremendous interest as catalysts in recent times. Bimetallic NPs are typically formed to lower the cost of a catalyst (An and Somorjai 2015; Shao et al. 2006) and/or to raise a monometal catalyst's characteristics (Dimitratos et al. 2012; Yang et al. 2012a, b). Maximum bimetallic NPs consist of a transition metal and a precious metal such as Au, and Pt, and a 3d transition metal involving Fe, Co, Ni, or Cu (An and Somorjai 2015; Yang et al. 2012a, b). These kinds of particles are used to catalyze several reactions including oxidation (Pritchard et al. 2010; Alhumaimesset al.2012; Balcha et al. 2011) and hydrogenation (Liuet al. 2016). The advantages of using bimetallic NPs as catalysts due to their vast surface area and tuning effect increase the number of active sites on which reaction can take place, as a result, increases the rate of a reaction (Balcha et al. 2011).

Recently, the noble bimetallic catalyst such as Au–Pd, Au–Ag, Au–Ni, Cu–Ni, and Ni–Co have been stated to be highly catalytic active in selective benzyl alcohol oxidation to benzaldehyde under moderate conditions (Sun et al. 2017; Alshammari et al. 2017; Liu et al. 2018; Kimi et al.2018). Furthermore, metal NPs based on noble metals (Pt, Pd, Au, etc.) have shown the extraordinary activity for reduction of the nitro group using H_2, $NaBH_4$, $N_2H_4{\cdot}H_2O$, etc. conditions (Zhang et al. 2016; Wuet al. 2012).

Noticeably, dendritic ligands based on diazine, particularly pyrimidine, have been drawn among other dendritic molecules owing to cheap cost, selective molecular reactivity recognition, and synthetic versatility (Yagai et al. 2019; Vollhardt et al. 2005). Most notably, pyrimidine's molecular recognition can define certain molecules through donation and acceptance of hydrogen bonds, metal chelation, and interactions with π–π. This capability has enabled many supramolecular structures and various forms of attractive oligomers and polymers that are needed to support metal nanoparticles (Vollhardt et al. 2005; Zimmerman and Lawless 2001). Low-priced bimetallic nickel–copper NPs catalytic systems supported by pyrimidine-based dendritic ligand make recyclable and reusable catalysts, minimizing particulate leaching relative to other costly metal NPs such as palladium, gold, platinum, etc. assisted by other ligands. These are crucial challenges from the eco, economic, and safety perspectives (Chalker et al. 2009; Chatterjee and Ward 2016).

Moreover, dendrimers are effective stabilizers in NPs' formation as they stabilize the nanoparticles through steric effects and create the NPs surface availability for catalytic reactions and also form size-specific dispersed NPs (Islam and Khan 2019). Also, the dendritic ligands can prevent agglomeration during the catalytic run and avoid oxidation of the sensitive active metal surface and enhance the catalytic activity of nanoparticles (Islam and Khan 2020).

However, such noble metals are expensive as rare supplies, and, nevertheless their extraordinary specificities, the high price of noble metals creates unattractive to use as a catalyst. This paved the way for developing the most effective, cheap, non-noble nanometal-based catalysts which will be immensely profitable (Rezaei et al. 2018; Lee et al. 2010). In recent times, Ni-based bimetallic NPs such as Ni–Cu, Ni–Co, and Ni–Sn were applied as an extremely active catalyst in the various reactions (Sharma et al. 2019).

Herein, we have studied rapid chemo-selective oxidation of alcohol into aldehyde and reduction of the nitro group into the amino group in the presence of another sensitive group of the same compound in the presence of water as solvent catalyzed by the more active dendritic ligand supported Ni/Cu (3:1) **4c** bimetallic NPs than other Ni/Cu (1:1) **4a** and Ni/Cu (1:3)**4b** at room temperature under green reaction conditions. The Ni/Cu (3:1) 4c bimetallic NPs were found as a heterogeneous catalyst and can be recycled at least five consecutive runs without any loss of activity.

Experimental section

Materials

All reagents are reagent graded and used without purification unless otherwise stated. Reaction solvent was deionized water used in the experiment. All the used reagents 2,4,6-Triaminopyrimidine (97%), 4-Chlorobenzoyl chloride (99%), Benzyl alcohol (anhydrous, 99.8%), 4-Methylbenzyl alcohol (98%), 4-Chlorobenzyl alcohol (99%), 4-Fluorobenzyl alcohol (97%), Furfuryl alcohol (98%), 2-Thiophenemethanol (98%), 1-(p-Tolyl)ethanol (≥ 97.0%), 1-(4-chlorophenyl) ethanol (98%), 1-(4-(hydroxymethyl)phenyl)ethanol (98%), 4-Nitrophenol (≥ 99%), Nitrobenzene (99%), 2-Nitrobenzaldehyde (98%), 4-nitrobenzoic acid (98%), 4-nitrobenzaldehyde (98%), 1-azido-4-nitrobenzene (98%), methyl 4-nitrobenzoate (99%), 1-Fluoro-4-nitrobenzene (99%), Copper(I) iodide (98%), Hydrazine monohydrate (reagent grade, 98%), Nickel(II) chloride hexahydrate (99.9% trace metals basis) from Sigma-Aldrich/Merck, USA, and

1-(4-nitrophenyl) ethanone (98%), 1-nitro-4-thiocyanatobenzene (98%) from Finetech Industry Limited, England, and also 2-(p-Tolyl)ethanol (98.0 + %) from TCI America, USA were purchased.

Methods

A melting point system (Model BUCHI, B-540) was used to calculate melting points through open capillary tubes. Purification of dendritic ligand and other products was performed by silica gel column chromatography on silica gel 60 N (neutral, 40–100 μM). Analytical thin-layer chromatography (TLC) of silica gel 60 F254 coated on 25 TCC aluminum sheets (20 × 20 cm) was used to monitor the reaction. Shimadzu's new-generation GC-2025 capillary gas chromatography was used to measure the percentage of conversion of alcohol and different substituted aromatic nitro compounds. The Shimadzu FT-IR 8400S Fourier Transform Infrared spectrophotometer was used to detect the IR spectra with KBr pellets (400–4000 cm^{-1}). ^{1}H NMR (400 MHz, Bruker) and ^{13}C NMR (100 MHz, Bruker) were recorded at 400 MHz and 100 MHz, respectively. Chemical shifts related to TMS were calculated. Elemental analyses of dendritic ligand and all solid products were carried out with a Fisons EA 1108 CHNS-O apparatus. JEOL-JSM-7600F was used to take surface morphology and elemental composition of all Ni/Cu of bimetallic NPs through SEM and EDX investigation. The X-RAY FLUORESCENCE (XRF) analysis to study the ratio of the metal composition of all Ni/Cu NPs was carried out by LAB CENTER XRF-1800 SEQUENTIAL X-RAY FLUORESCENCE SPECTROMETER. The TEM analysis of all nanoparticles was done by Thermo Scientific Talos F200X Transmission Electron Microscope (TEM) to measure the average nanosize of the particles and phase was observed by a PANANALYTICAL X-ray diffractometer (XRD). Perkin Elmer ELAN DRC E ICP/MS was used to study the leaching of Ni and Cu after a catalytic run of the Ni/Cu NPs catalyst.

Synthesis and characterization of dendritic ligand 2,4,6-Tris (di-4-chlorobenzamido)-1,3-diazine (3) and Ni/Cu (1:1) 4a, Ni/Cu (1:3) 4b, and Ni/Cu (3:1) 4cbimetallic NPs

Dendritic ligand 2,4,6-tris (di-4-chlorobenzamido)-1,3-diazine (3)

In a round-bottom flask, the mixture of 2,4,6-triaminopyrimidine (0.2 g, 0.00159 mmol) **1** and 4-Chlorobenzoyl chloride **2** (3 mL, 9.50 mmol) was introduced in 10 mL of DMF was stirred at 90 °C temperature for 9 h. The reaction advancement was observed by thin-layer chromatography (TLC). After the complete reaction reactants, distilled water was added and the crude product was extracted with $CHCl_3$. After removing the solvent under reduced pressure, the crude product was run through silica gel column chromatography (n-hexane/ethylacetate 1:8). Finally, the dendritic product (3) was obtained after further purification by recrystallization with ethanol.

White crystalline solid, 90% yield, mp. 308–310 °C, Mol. Wt.: 956.44, IR (KBr): μ_{max} (cm^{-1}) 3094.89, 1680.20, 1592.29, 1424.489, 1092.71, 780.20. ^{1}H NMR (400 MHz, $CDCl_3$): δ_H (ppm) 4.62 (s, 1H, Ar–H), 7.65 (d, 12H, $J = 8.8$ Hz, Ar–H), 8.28 (d, 12H, $J = 8.8$ Hz, Ar–H). ^{13}C NMR (100 MHz, $CDCl_3$): δ_C (ppm) 71.88, 126.65, 129.62, 133.25, 138.25, 167.24, 170.16, 172.42. Anal. Calcd. for $C_{46}H_{25}Cl_6N_5O_6$: C, 57.77; H, 2.63; N, 7.32; Found: C, 57.70; H, 2.60; N, 7.30.

Synthesis of Ni/Cu (1:1) 4a, Ni/Cu (1:3) 4b, and Ni/Cu (3:1) 4c bimetallic NPs by co-complexation method

General procedure—nickel chloride (0.5 g, 0.0038 M) and copper iodide (0.734 g, 0.0038 M) (molar ratio 1:1)/0.0038 M nickel chloride (0.5 g) and 0.0114 M copper iodide (2.204 g) (molar ratio 1:3)/nickel chloride (1.020 g, 0.0078 M) and copper iodide (0.5 g, 0.00262 M) (molar ratio 3:1) were dissolved and stirred separately in 10 mL ethanol containing dendritic ligand **3** (0.5 g) in three R.B flask by the addition of 10 mL hydrazine hydrate. A few drops of 1 M KOH were introduced with continuous stirring for maintaining pH = 11.0, and then, the temperature of the reaction mixture was maintained at 120 °C for 2 h. The precipitation of these bimetallic nanoparticles was separated, washed with ethanol, and dried at 100 °C overnight.

General procedure for the selective oxidation of alcohol to the aldehyde using Ni/Cu (3:1) 4c bimetallic NPs as a catalyst

In a round-bottom flask, alcohol (1.0 mmol) and Ni/Cu (3:1) **4c** of 4.0 mol% catalyst were added to water (5.0 mL) and the mixture was stirred for 30 min at room temperature. The reaction progress and conversion of the reactants were monitored by gas chromatography (GC). The reaction mixture was centrifuged at 4,000 rpm after the complete conversion of alcohol into aldehyde or ketone due to isolating the catalyst and was filtered. Finally, the desired pure products were obtained from the run through silica gel column chromatography (n-hexane/ethylacetate 10:1).

Benzaldehyde (13) (Pan et al. 2018)

Colorless oil, 90% yield (Table 3, entry 1), ^{1}H NMR ($CDCl_3$, 400 MHz): δ_H (ppm) 7.52–7.68 (m, 3H, Ar–H); 8.10 (d, 2H, $J = 8.8$ Hz, Ar–H); 9.18 (s, 1H, CHO).

4-Methylbenzaldehyde (14) (Pan et al. 2018)

Colorless oil, 94% yield (Table 3, entry 2), Mol. Wt.: 120.15,^{1}H NMR ($CDCl_3$, 400 MHz): δ_H (ppm) 2.62 (s, 3H, CH_3); 7.76 (d, 2H, $J = 8.0$ Hz, Ar–H); 8.69 (d, 2H, $J = 8.0$ Hz, Ar–H); 9.88 (s, 1H, CHO). ^{13}C NMR ($CDCl_3$, 100 MHz): δ_C (ppm) 25.45, 129.33, 129.47, 135.20, 144.24, 191.07.

2-p-Tolylacetaldehyde (15)

Colorless oil, 85% yield (Table 3, entry 3), Mol. Wt.: 134.18, ^{1}H NMR ($CDCl_3$, 400 MHz): δ_H (ppm) 2.20 (s, 3H, CH_3), 3.76 (d, 2H, $J = 8.0$ Hz, CH_2); 6.98 (s, 4H, Ar–H); 9.87 (t, 1H, $J = 4.0$ Hz, CHO). ^{13}C NMR ($CDCl_3$, 100 MHz): δ_C (ppm) 25.00, 50.00, 129.00, 134.44, 137.24, 200.24.

4-Chlorobenzaldehyde (16) (Pan et al.2018)

Colorless solid, 84% yield (Table 3, entry 4), mp. 45–47 °C (lit. 44–46 °C), Mol. Wt.: 140.57, ^{1}H NMR ($CDCl_3$, 400 MHz): δ_H (ppm) 7.79 (d, 2H, $J = 8.0$ Hz, Ar–H); 8.16 (d, 2H, $J = 8.0$ Hz, Ar–H); 9.87 (s, 1H, CHO). ^{13}C NMR ($CDCl_3$, 100 MHz): δ_C (ppm) 129.00, 132.44, 135.45, 140.54, 192.00. Anal. Calcd. for C_7H_5ClO: C, 59.81; H, 3.59; Found: C, 59.78; H, 3.50.

4-Fluorobenzaldehyde (17) (Pan et al. 2018)

Colorless oil, 82% yield (Table 3, entry 5), Mol. Wt.: 124.11, ^{1}H NMR ($CDCl_3$, 400 MHz): δ_H (ppm) 6.89 (d, 2H, $J = 8.0$ Hz, Ar–H); 7.59 (d, 2H, $J = 8.4$ Hz, Ar–H); 9.86 (s, 1H, CHO). ^{13}C NMR ($CDCl_3$, 100 MHz): δ_C (ppm) 116.72, 130.43, 133.43, 167.74, 192.23.

(Z)-3,7-Dimethylocta-2,6-dienal (18)

Colorless oil, 80% yield (Table 3, entry 6), Mol. Wt.: 152.23, ^{1}H NMR ($CDCl_3$, 400 MHz): δ_H (ppm) 1.30 (s, 9H, CH_3); 2.01 (d, 4H, $J = 7.6$ Hz, CH_2); 5.00 (s, 1H, CH), 5.63 (d, 1H, $J = 0.4$ Hz, CH); 9.86 (d, 1H, $J = 0.4$ Hz, CHO). ^{13}C NMR ($CDCl_3$, 100 MHz): δ_C (ppm) 19.40, 22.40, 25.79, 33.46, 123.13, 128.24, 132.56, 164.07, 192.07.

Furan-2-carbaldehyde (19) (Pan et al. 2018)

Yellow oil, 82% yield (Table 3, entry 7), Mol. Wt.: 96.08,^{1}H NMR ($CDCl_3$, 400 MHz):δ_H (ppm) 6.45 (t, 1H, $J = 7.6$ Hz, Ar–H); 7.89 (d, 1H, $J = 4.8$ Hz, Ar–H); 8.10 (d, 1H, $J = 4.8$ Hz, Ar–H); 9.99 (s, 1H, CHO). ^{13}C NMR ($CDCl_3$, 100 MHz): δ_C (ppm) 112.00, 121.70, 149.94, 153.22, 178.24.

Thiophene-2-carbaldehyde (20) (Pan et al. 2018)

Yellow oil, 81% yield (Table 3, entry 8), Mol. Wt.: 112.15, ^{1}H NMR ($CDCl_3$, 400 MHz):δ_H (ppm) 6.30 (t, 1H, $J = 8.0$ Hz, Ar–H); 7.38–7.43 (m, 2H, Ar–H); 9.50 (s, 1H, CHO). ^{13}C NMR ($CDCl_3$, 100 MHz): δ_C (ppm) 127.70, 135.35, 137.32, 143.23, 182.24.

1-p-Tolylethanone (23)

Colorless liquid, 86% yield (Table 4, entry 1), Mol. Wt.: 134.18,^{1}H NMR ($CDCl_3$, 400 MHz):δ_H (ppm) 2.37 (s, 3H, CH_3); 2.72 (s, 3H, CH_3); 7.76 (d, 2H, $J = 8.0$ Hz, Ar–H); 8.79 (d, 2H, $J = 8.0$ Hz, Ar–H). ^{13}C NMR ($CDCl_3$, 100 MHz): δ_C (ppm) 24.45, 28.46, 128.33, 129.94, 134.12, 142.24, 200.00.

1-(4-Chlorophenyl)ethanone (24) (Addis et al. 2010)

Colorless solid, 85% yield (Table 4, entry 2), mp. 75–77 °C, (lit. 74–76 °C), Mol. Wt.: 154.59,^{1}H NMR ($CDCl_3$, 400 MHz): δ_H (ppm) 2.28 (s, 3H, CH_3); 2.72 (s, 3H, CH_3); 7.67 (d, 2H, $J = 7.6$ Hz, Ar–H); 8.10 (d, 2H, $J = 8.8$ Hz, Ar–H). ^{13}C NMR ($CDCl_3$, 100 MHz): δ_C (ppm) 30.00, 129.00, 130.00, 134.54, 137.34, 200.33.Anal. Calcd. for C_8H_7ClO: C, 62.15; H, 4.56; Found: C, 62.15; H, 4.56.

4(1-Hydroxyethyl)benzaldehyde (26) (Jiang and Ma 2018)

.Colorless oil, 82% yield (Table 5, entry 2), Mol. Wt.: 150.17, ^{1}H NMR ($CDCl_3$, 400 MHz): δ_H (ppm) 1.61 (s, 3H, CH_3); 2.11 (s, 1H, OH); 4.42–4.50 (m, 1H, CH), 7.76 (d, 2H, $J = 8.0$ Hz, Ar–H); 8.69 (d, 2H, $J = 8.0$ Hz, Ar–H); 9.89 (s, 1H, CHO). ^{13}C NMR ($CDCl_3$, 100 MHz): δ_C (ppm) 22.77, 75.76, 116.76, 120.14, 130.23, 152.24, 166.24.

General procedure for the selective reduction of the nitro group of different compounds using Ni/Cu (3:1) 4c bimetallic NPs as a catalyst

In a round-bottom flask, 1.0 mmol of the nitro substrate was provided in 5 ml of distilled water. By adding 0.5 mmol hydrazine hydrate and catalyst Ni/Cu (3:1) **4c** of 4.0 mol% to this solution and stirring the reaction mixture at room temperature for 20 min. Gas chromatography (GC) was used to observe the movement of the reaction and to detect the conversion of the reactants. The reaction mixture was centrifuged at 4,000 rpm after completion of the reaction and filtered to isolate the catalyst. Eventually, from the run through silica gel column chromatography (n-hexane/ethylacetate 10:1), the targeted pure products were collected.

4-Aminophenol (37)

White solid, 96% yield (Table 7, entry 1), mp. 182–184 °C (lit. 181–183 °C) (Takasaki et al. 2008).

Mol. Wt.: 109.13, ^{1}H NMR ($CDCl_3$, 400 MHz): δ_H (ppm) 4.00 (s, 2H, NH_2); 5.20 (s, 1H, OH); 6.16–6.19 (dd, 2H, $J = 4.0$, 2.0 Hz); 6.45–6.48 (dd, 2H, $J = 6.8$, 4.0 Hz). ^{13}C NMR ($CDCl_3$, 100 MHz): δ_C (ppm) 17.74, 118.84, 141.13, 148.43. Anal. Calcd. for C_6H_7NO: C, 66.04; H, 6.47; N, 12.84; Found: C, 66.00; H, 6.40; N, 12.81.

Aniline (38)

Colorless liquid, 88% yield (Table 7, entry 2), Mol. Wt.: 93.13, ^{1}H NMR (400 MHz): δ_H (ppm) 4.00(s, 2H, NH_2); 7.16 (d, 2H, $J = 4.0$ Hz); 7.41–7.56 (m, 1H); 8.04 (d, 2H, $J = 8.0$ Hz).

2-Aminobenzaldehyde (39) (Reddy et al. 2015)

Yellow solid, 97% yield (Table 7, entry 3), mp. 33–35 oC, (Lit. 32–34 °C).

Mol. Wt.: 121.14, ^{1}H NMR ($CDCl_3$, 400 MHz): δ_H (ppm) 4.00 (s, 2H, NH_2); 6.86 (d, 1H, $J = 2.8$ Hz); 7.40 (t, 1H, $J = 5.6$ Hz); 7.70 (d, $J = 4.0$, 1H); 10.40 (s, 1H, CHO). ^{13}C NMR ($CDCl_3$, 100 MHz): δ_C (ppm) 117.34, 119.00, 130.23, 131.34, 135.12, 150.23, 200.00. Anal. Calcd. for C_7H_7NO: C, 69.41; H, 5.82; N, 11.56; Found: C, 69.39; H, 5.78; N, 11.50.

4-Aminobenzoic acid (40) (Takasaki et al. 2008)

White–gray crystals, 91% yield (Table 7, entry 4), mp. 188–190 °C (Lit. 187–189 °C), Mol. Wt.: 137.14, ^{1}H NMR ($CDCl_3$, 400 MHz): δ_H (ppm) 4.11 (s, 2H, NH_2); 6.66 (d, 2H, $J = 4.0$ Hz, Ar–H); 7.76 (d, 2H, $J = 8.4$ Hz, Ar–H); 10.88 (s, 1H, COOH). ^{13}C NMR ($CDCl_3$, 100 MHz): δ_C (ppm) 116.33, 120.47, 132.33, 153.14, 170.24. Anal. Calcd. for $C_7H_7NO_2$: C, 61.31; H, 5.14; N, 10.21, Found: C, 61.28; H, 5.11; N, 10.18.

4-Aminobenzaldehyde (41) (Sharif et al. 2014)

Yellow solid, 96% yield (Table 7, entry 5), mp. 34–36 oC, (Lit. 33–35 °C), Mol. Wt.: 121.14, ^{1}H NMR ($CDCl_3$, 400 MHz): δ_H (ppm) 4.12 (s, 2H, NH_2); 6.46 (d, 2H, $J = 4.0$ Hz, Ar–H); 7.46 (d, 2H, $J = 4.4$ Hz, Ar–H); 9.88 (s, 1H, CHO). ^{13}C NMR ($CDCl_3$, 100 MHz): δ_C (ppm) 116.78, 126.67, 130.34, 154.44, 160.24, 190.24. Anal. Calcd. for C_7H_7NO: C, 69.41; H, 5.82; N, 11.56; Found: C, 69.38; H, 5.79; N, 11.51.

4-Azidobenzenamine (42) (Pagoti et al.2013)

Brown crystalline solid, 93% yield (Table 7, entry 6), mp. 164–166 °C (Lit. 165 °C), Mol. Wt.: 134.14, ^{1}H NMR ($CDCl_3$, 400 MHz): δ_H (ppm) 4.00 (s, 2H, NH_2); 6.45 (d, 2H, $J = 8.8$ Hz, Ar–H); 7.63 (d, 2H, $J = 8.0$ Hz, Ar–H). ^{13}C NMR ($CDCl_3$, 100 MHz): δ_C (ppm) 166.66, 130.23, 136.22, 149.24. Anal. Calcd. for $C_6H_6N_4$: C, 53.72; H, 4.51; N, 41.77; Found: C, 53.70; H, 4.49; N, 41.70.

Methyl 4-aminobenzoate (43) (Takasaki et al. 2008)

Slightly brown crystalline solid, 91% yield (Table 7, entry 7), mp. 101–102 °C (Lit. 102–103 °C); Mol. Wt.: 151.16, ^{1}H NMR ($CDCl_3$, 400 MHz): δ_H (ppm) 3.66 (s, 3H, CH_3), 4.16 (s, 2H, NH_2); 6.66 (d, 2H, $J = 4.0$ Hz, Ar–H); 7.75 (d, 2H, $J = 8.0$ Hz, Ar–H). ^{13}C NMR ($CDCl_3$, 100 MHz): δ_C (ppm) 50.77, 116.76, 120.14, 130.23, 152.24, 166.23. Anal. Calcd. for $C_8H_9NO_2$: C, 63.56; H, 6.00; N, 9.27; Found: C, 63.50; H, 5.98; N, 9.21.

1-(4-Aminophenyl)ethanone (44) (Currall and David Jackson 2014)

Brown crystalline solid, 93% yield (Table 7, entry 8), mp. 104–106 °C, (Lit. 103–105 °C), Mol. Wt.: 135.6, ^{1}H NMR ($CDCl_3$, 400 MHz): δ_H (ppm) 2.56 (s, 3H, CH_3), 4.26 (s, 2H, NH_2); 6.56 (d, 2H, $J = 4.0$ Hz, Ar–H); 7.66 (d, 2H, $J = 8.0$ Hz, Ar–H). ^{13}C NMR ($CDCl_3$, 100 MHz): δ_C (ppm) 30.77, 116.78, 127.77, 130.24, 152.14, 160.24.

Anal. Calcd. for C_8H_9NO: C, 71.09; H, 6.71; N, 10.36; Found: C, 71.00; H, 6.69; N, 10.30.

4-Thiocyanatobenzenamine (45)

Brown crystalline solid, 95% yield (Table 7, entry 9), mp. 115–117 °C, Mol. Wt.: 150.2**,** ^{1}H NMR ($CDCl_3$, 400 MHz): δ_H (ppm) 4.04 (s, 2H, NH_2); 6.20 (d, 2H, $J = 8.0$ Hz, Ar–H); 6.73 (d, 2H, $J = 8.0$ Hz, Ar–H). ^{13}C NMR ($CDCl_3$, 100 MHz): δ_C (ppm) 112.33, 114.47, 117.77, 132.24, 151.14. Anal. Calcd. for $C_7H_6N_2S$.

: C, 55.97; H, 4.03; N, 18.65; S, 21.35, Found: C, 55.90; H, 4.00; N, 18.61; S, 21.31.

4-Fluorobenzenamine (46) (Ishikawa 1994)

Oily Liquid, 87% yield (Table 7, entry 10), Mol. Wt.: 111.12, ^{1}H NMR ($CDCl_3$, 400 MHz): δ_H (ppm) 4.10 (s, 2H, NH_2); 6.13–6.20 (m, 2H, Ar–H); 6.45–6.58 (m, 2H, Ar–H). ^{13}C NMR ($CDCl_3$, 100 MHz): δ_C (ppm) 116.76, 117.76, 142.23, 152.14.

Results and discussion

Synthesis and characterization of dendritic ligand 2,4,6-Tris (di-4-chlorobenzamido)-1,3-diazine (3)

Dendritic ligand 2,4,6-Tris (di-4-chlorobenzamido)-1,3-diazine (**3**) was prepared with a reaction of 2,4,6-Triamino-pyrimidine (**1**), 4-chlorobenzoyl chloride (**2**) in anhydrous DMF at 90 °C for 9 h (Scheme 1) (Islam and Khan 2019). The product (**3**) was analyzed by IR, ^{1}H NMR, ^{13}C NMR, and elemental analysis.

In the IR spectrum of dendritic ligand (**3**) (S1 in the supplementary information), the band at 3094.89 cm^{-1} and 1592.29 cm^{-1} indicates the C-H (aro) and C=N (aro) stretching absorption, respectively, while the bands at 1424.48 cm^{-1} and 1092.71 cm^{-1} stretching bands specify the existence of C=C (aro) and C–N (aro) correspondingly. Particularly, the sharp band at 1620.20 cm^{-1} and 780.20 cm^{-1} signifies the C=O group and the aromatic C–Cl bond individually. Also, the ^{1}H NMR (S2 in the supplementary information), and ^{13}C NMR spectrum (S3 in the supplementary information), as well as elemental analysis, confirms the formation of compound (**3**).

Synthesis and characterization of Ni/Cu (1:1) 4a, Ni/Cu (1:3) 4b, and Ni/Cu (3:1) 4c bimetallic NPs supported by dendritic ligand 2,4,6-Tris (di-4-chlorobenzamido)-1,3-diazine (3)

Dendritic ligand 2,4,6-Tris (di-4-chloro benzamido)-1,3-diazine supported Ni/Cu (1:1) **4a** bimetallic NPs were prepared by adding $NiCl_2{\cdot}6H_2O$:CuI (1:1) to the ligand (**3**) in the presence of $NH_2.NH_2.H_2O$ and KOH in ethanol at 120 °C for 2 h with stirring the reaction mixture.

Similarly, 2,4,6-Tris (di-4-chlorobenzamido)-1,3-diazine-supported Ni/Cu (1:3) **4a** bimetallic NPs were prepared by introducing $NiCl_2{\cdot}6H_2O$: CuI (1:3) to the ligand (**3**) in the presence of $NH_2{\cdot}NH_2{\cdot}H_2O$ and KOH in ethanol at 120 °C for 2 h with stirring.

Also, 2,4,6-Tris (di-4-chloro benzamido)-1,3-diazine-supported Ni/Cu (3:1) **4a** bimetallic NPs were synthesized by loading $NiCl_2{\cdot}6H_2O$: CuI (3:1) to the ligand (**3**) in the presence of $NH_2.NH_2.H_2O$ and KOH in ethanol at 120 °C for 2 h with stirring.

However, the dendritic ligand 2,4,6-Tris (di-4-chlorobenzamido)-1,3-diazine (**3**) assisted Ni/Cu bimetallic NPs of different molar ratios (1:1**4a**, 1:3**4b**, and 3:1**4c**) were synthesized by co-complexation method (Schemes 2, 3, 4) and also described by particular physicochemical methods such as SEM, EDX, XRF, TEM, and XRD. The SEM images of surface morphology of all Ni/Cu bimetallic NPs **4a, 4b,** and **4c** display almost similar aggregated globular size of the particle as well as the dendritic shape (Figs. 1, 2, 3).

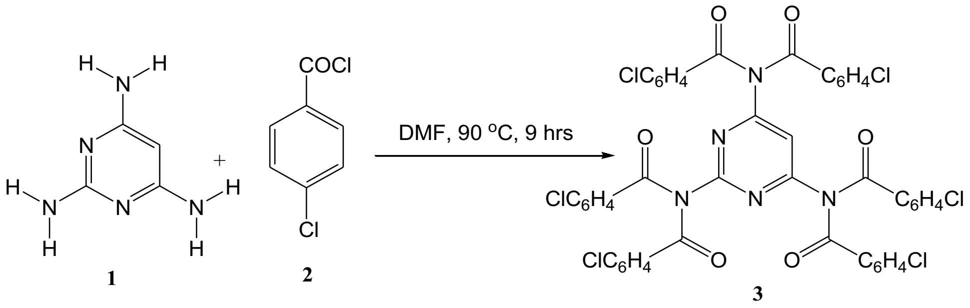

Scheme 1 Synthesis of 2,4,6-Tris (di-4-chlorobenzamido)-1,3-diazine (**3**)

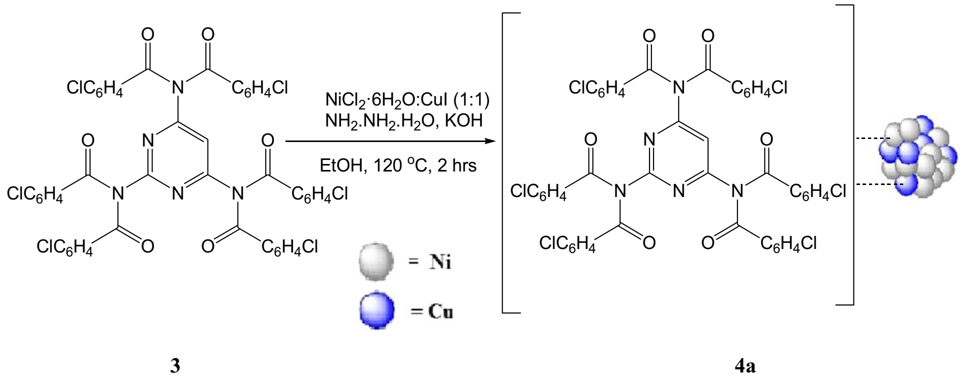

Scheme 2 Synthesis of 2,4,6-Tris (di-4-chlorobenzamido)-1,3-diazine supported Ni/Cu (1:1) **4a** bimetallic NPs

Scheme 3 Synthesis of 2,4,6-Tris (di-4-chlorobenzamido)-1,3-diazine supported Ni/Cu (1:3) **4b** bimetallic NPs

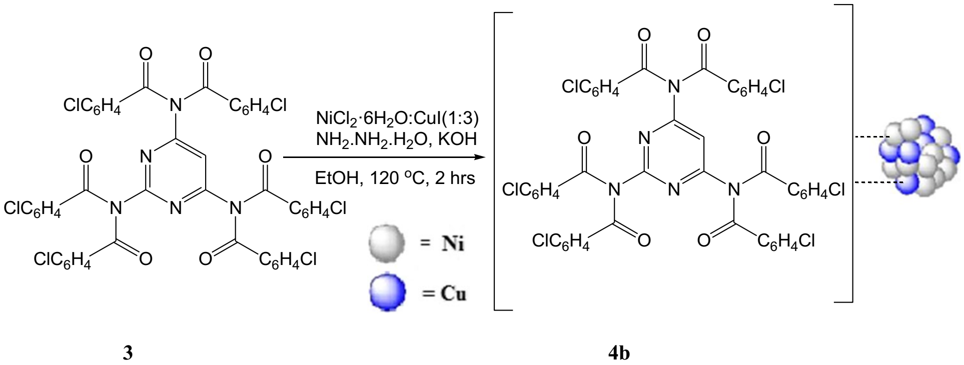

Scheme 4 Synthesis of 2,4,6-Tris (di-4-chlorobenzamido)-1,3-diazine supported Ni/Cu (3:1) **4c** bimetallic NPs

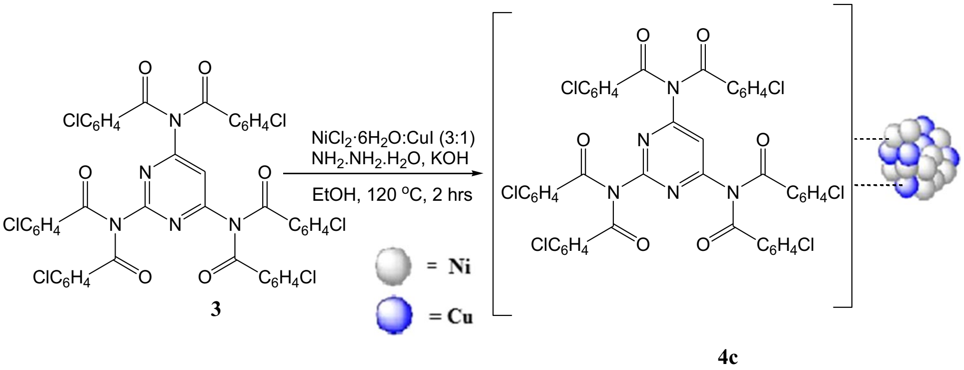

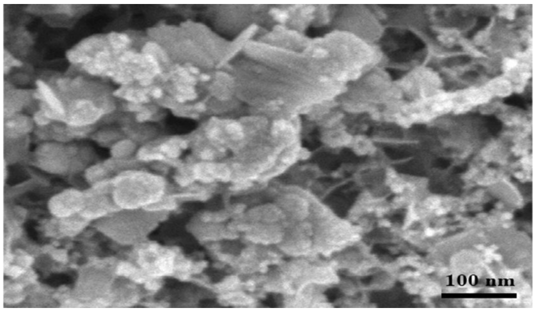

Fig. 1 SEM of Ni/Cu (1:1) **4a**

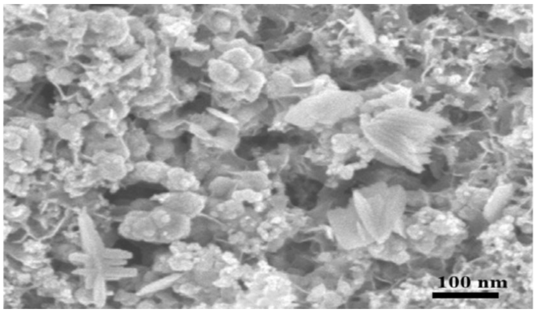

Fig. 3 SEM of Ni/Cu (3:1) **4c**

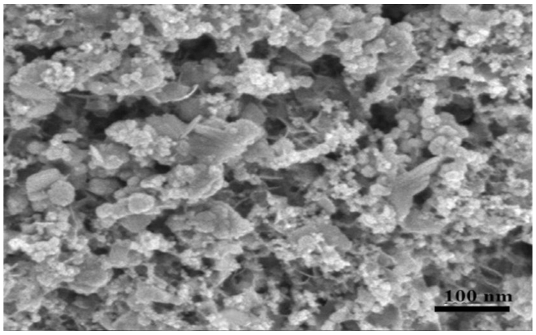

Fig. 2 SEM of Ni/Cu (1:3) **4b**

The investigated EDX results of these synthesized Ni/Cu bimetallic NPs have established the formation of the three different molar ratios of nanoparticles. Figure 4 exhibits the elemental composition, i.e., copper (40.69% of mass) and nickel (39.80%% of mass) that specifies the formation of Ni/Cu (1:1) **4a** bimetallic NPs. Likewise, Fig. 5 displays the amount of copper (17.12% of mass) and nickel (5.82% of mass) that indicates the creation of Ni/Cu (1:3) **4b** NPs**.** Similarly, Fig. 6 shows the amount of element nickel (17.82% of mass) and copper (5.12% of mass) that confirms the growth of Ni/Cu (3:1) **4c**.

However, Table 1 demonstrates the observed XRF results of the synthesized three different Ni/Cu (1:1) **4a**, Ni/Cu (1:3) **4b**, and Ni/Cu (3:1) **4c** bimetallic NPs which supports the

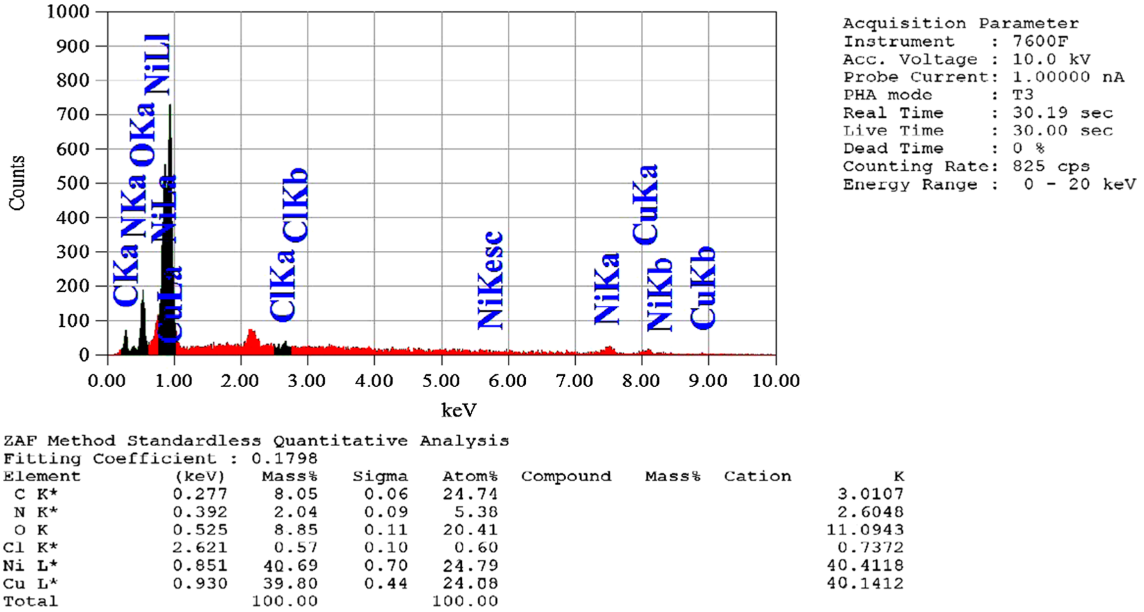

```
Acquisition Parameter
Instrument    : 7600F
Acc. Voltage  : 10.0 kV
Probe Current: 1.00000 nA
PHA mode      : T3
Real Time     : 30.19 sec
Live Time     : 30.00 sec
Dead Time     : 0 %
Counting Rate: 825 cps
Energy Range :  0 - 20 keV
```

```
ZAF Method Standardless Quantitative Analysis
Fitting Coefficient : 0.1798
Element         (keV)   Mass%   Sigma   Atom%  Compound   Mass%  Cation         K
 C K*           0.277    8.05    0.06   24.74                                3.0107
 N K*           0.392    2.04    0.09    5.38                                2.6048
 O K            0.525    8.85    0.11   20.41                               11.0943
Cl K*           2.621    0.57    0.10    0.60                                0.7372
Ni L*           0.851   40.69    0.70   24.79                               40.4118
Cu L*           0.930   39.80    0.44   24.08                               40.1412
Total                  100.00          100.00
```

Fig. 4 EDX analysis of Ni/Cu (1:1)**4a**

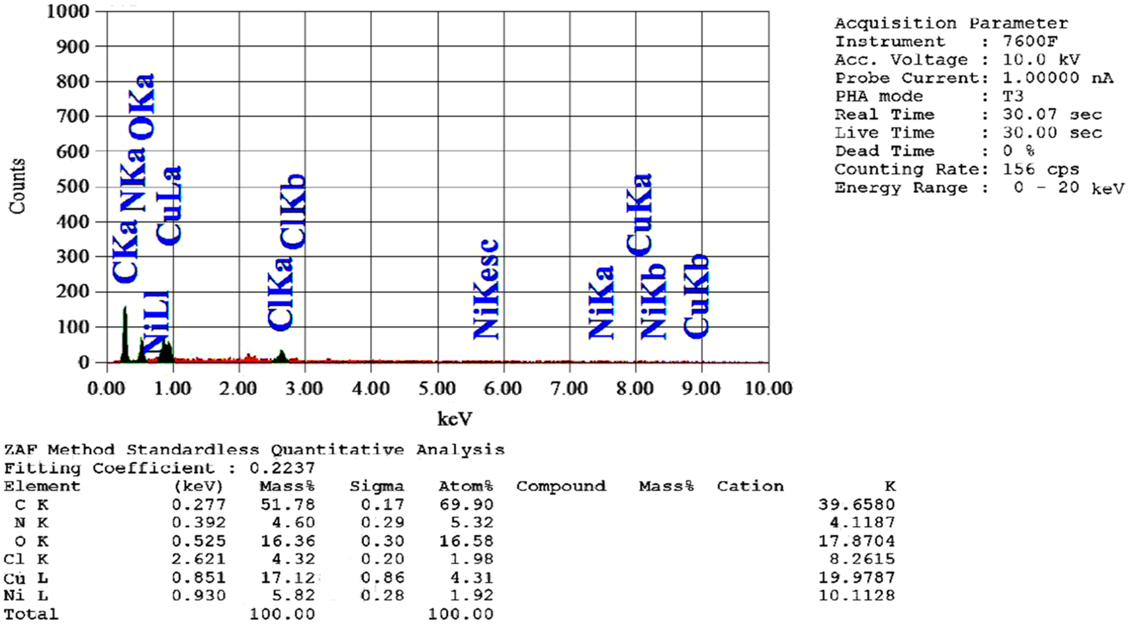

```
Acquisition Parameter
Instrument    : 7600F
Acc. Voltage  : 10.0 kV
Probe Current: 1.00000 nA
PHA mode      : T3
Real Time     : 30.07 sec
Live Time     : 30.00 sec
Dead Time     : 0 %
Counting Rate: 156 cps
Energy Range :  0 - 20 keV
```

```
ZAF Method Standardless Quantitative Analysis
Fitting Coefficient : 0.2237
Element         (keV)   Mass%   Sigma   Atom%  Compound   Mass%  Cation         K
 C K            0.277   51.78    0.17   69.90                               39.6580
 N K            0.392    4.60    0.29    5.32                                4.1187
 O K            0.525   16.36    0.30   16.58                               17.8704
Cl K            2.621    4.32    0.20    1.98                                8.2615
Cu L            0.851   17.12    0.86    4.31                               19.9787
Ni L            0.930    5.82    0.28    1.92                               10.1128
Total                  100.00          100.00
```

Fig. 5 EDX analysis of Ni/Cu (1:3)**4b**

EDX result of these NPs and confirms that the preparation method of these bimetallic NPs was successful.

Figure 7 presents that the peaks at 2 theta (2Θ) values of 36.20 and 61.30 degrees matching to the crystal planes of (111) and (220), respectively, compared with the International Center of Diffraction Data Card (JCPDS card 77–0199) for Cu_2O powder of X-ray diffraction analysis (Lee et al. 2010) have proven the existence of the single cubic cuprous oxide phase in the three Ni/Cu (1:1) **4a**, Ni/Cu (1:3) **4b**, and Ni/Cu (3:1) **4c** bimetallic NPs. Conversely, Fig. 7 shows that the nonappearance of any typical peaks of CuO of XRD patterns, suggesting that a pure cuprous oxide phase was formed in these NPs.

Also, Fig. 7 displays that the prominent XRD peaks at 43.50, 51.00, and 74.90 degrees relating to (111), (200), and (220) planes specify the FCC phase of Cu NPs (JCPDS card

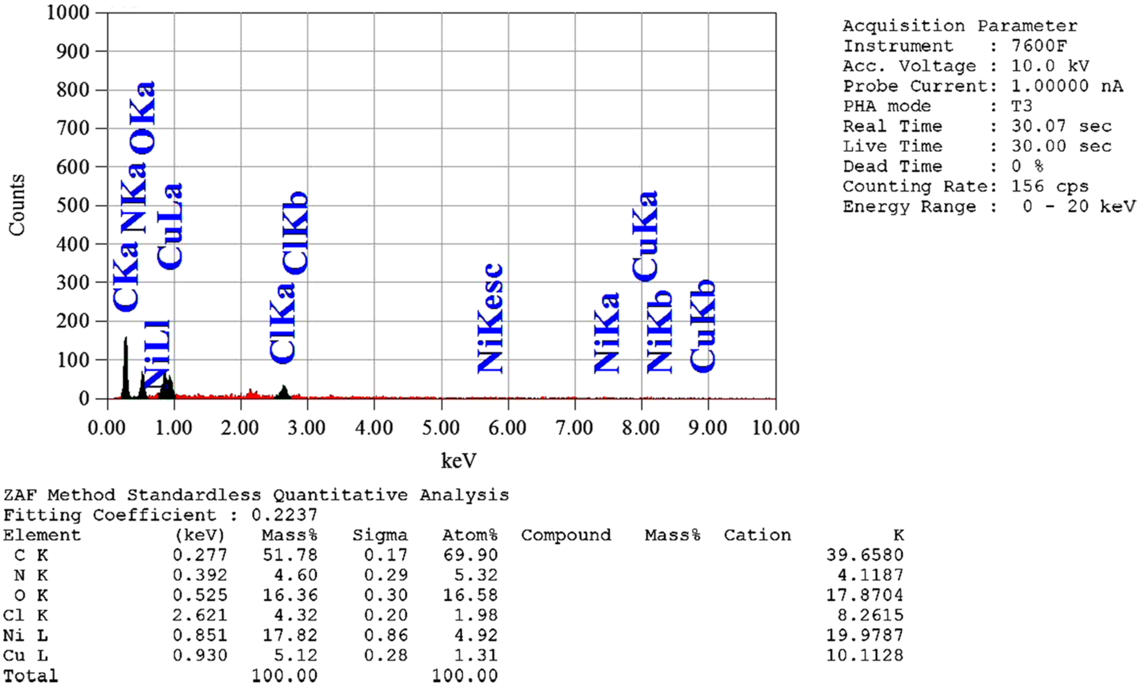

```
Acquisition Parameter
Instrument    : 7600F
Acc. Voltage : 10.0 kV
Probe Current: 1.00000 nA
PHA mode      : T3
Real Time     : 30.07 sec
Live Time     : 30.00 sec
Dead Time     : 0 %
Counting Rate: 156 cps
Energy Range :  0 - 20 keV
```

```
ZAF Method Standardless Quantitative Analysis
Fitting Coefficient : 0.2237
Element        (keV)   Mass%   Sigma   Atom%  Compound    Mass%  Cation          K
 C K           0.277   51.78    0.17   69.90                               39.6580
 N K           0.392    4.60    0.29    5.32                                4.1187
 O K           0.525   16.36    0.30   16.58                               17.8704
Cl K           2.621    4.32    0.20    1.98                                8.2615
Ni L           0.851   17.82    0.86    4.92                               19.9787
Cu L           0.930    5.12    0.28    1.31                               10.1128
Total                 100.00          100.00
```

Fig. 6 EDX analysis of Ni/Cu (3:1) **4c**

Table 1 Quantitative results of XRF analysis of three different Ni/Cu (1:1) **4a**, Ni/Cu (1:3) **4b**, and Ni/Cu (3:1) **4c** bimetallic NPs

Analytic metal	Result (w/w)% of Ni/Cu (1:1) **4a** bimetallic NPs (%)	Result (w/w)% of Ni/Cu (1:3) **4b** bimetallic NPs (%)	Result (w/w)% of Ni/Cu (3:1) **4c** bimetallic NPs (%)
Ni	50.2136	24.1135	74.7614
Cu	49.7864	75.8865	25.2386

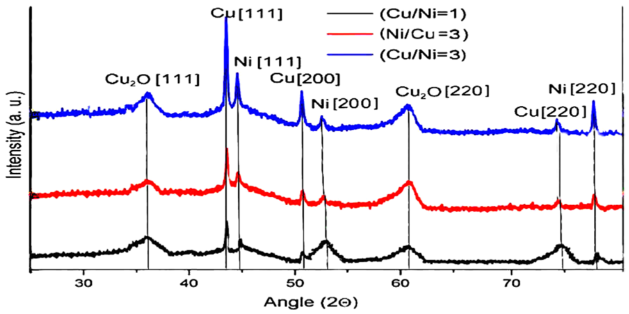

Fig. 7 XRD analysis of Ni/Cu (1:1) **4a**, Ni/Cu (1:3) **4b**, Ni/Cu (3:1) **4c** bimetallic NPs

no.85-1326) (Yang et al. 2017) in the three Ni/Cu (1:1) **4a**, Ni/Cu (1:3) **4b**, and Ni/Cu(3:1) **4c** bimetallic NPs. Furthermore, Fig. 7 demonstrates that the peaks at 2 theta values of 42.20, 51.00, and 74.15 degrees associating with (111), (200), and (220) nickel planes, respectively, those associated with the JCPDS General Powder Diffraction Card, Nickel Record No (04—0850) (File, 1997) reveal the growth of FCC nickel NPs (Yang et al. 2017).

Notably, Figs. 8 and 9 reveal the TEM analysis result that demonstrates the maximum number of the average size of the nanoparticles is 25–30 nm in the Ni/Cu (1:1) **4a** and Ni/Cu (1:3) **4b** bimetallic NPs, whereas Fig. 10 exhibit 15–20 nm average size of the nanoparticles in the Ni/Cu (3:1) **4c** bimetallic NPs.

Catalytic performance of Ni/Cu 4a, 4b, and 4c bimetallic NPs for the chemoselective oxidation of alcohol

Recently, various interesting studies of bimetallic NPs such as Cu–Ni NPs assisted on activated carbon (Kimi et al. 2018) and AuPd alloys embedded in MgO and MnO_2 (Alshammari et al. 2017), etc. for the chemoselective oxidation of alcohol into aldehyde have been done. Metal nanoparticle catalyzed high-temperature-based oxidation reaction of aromatic alcohol easily creates aromatic acid and ester due to over oxidation of aromatic aldehyde and decreases selective oxidation in the presence of another sensitive group and for this problem, we avoided high temperature and also another organic solvent.

However, the chemoselective oxidation of benzyl alcohol to benzaldehyde catalyzed by the Ni/Cu bimetallic nanoparticle (molar ratio 1:1/1:3/3:1) bimetallic NPs **4a, 4b, and 4c** was examined as a model reaction (Scheme 5) due to

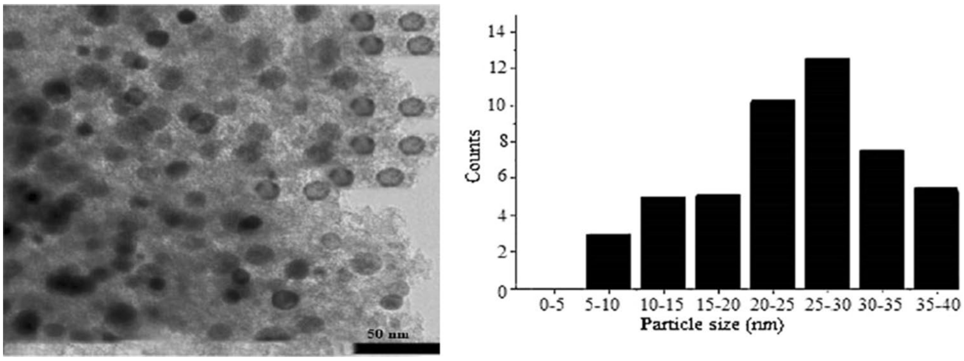

Fig. 8 TEM analysis of Ni/Cu (1:1) **4a** bimetallic NPs

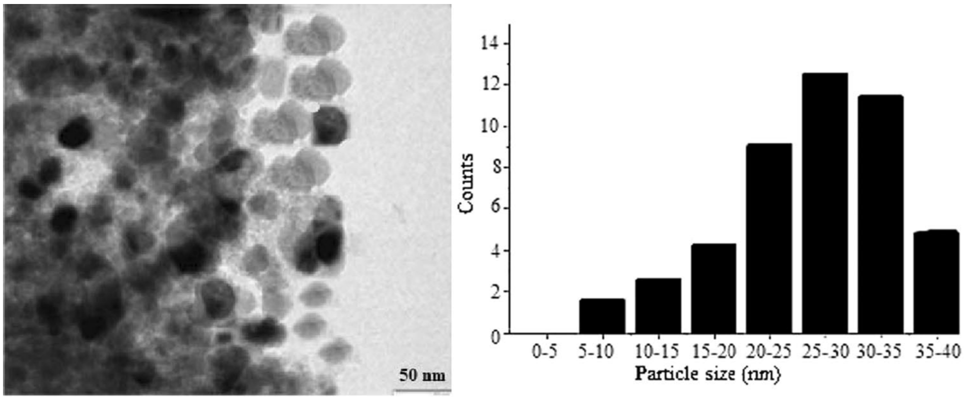

Fig. 9 TEM analysis of Ni/Cu (1:3) **4b** bimetallic NPs

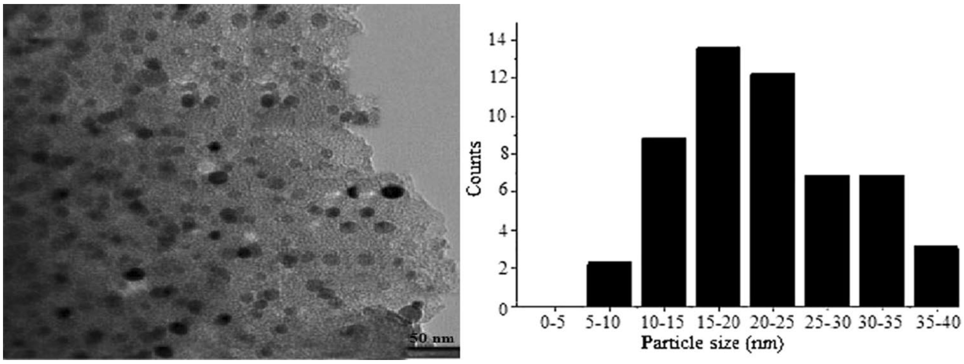

Fig. 10 TEM analysis of Ni/Cu (3:1) **4c** bimetallic NPs

the determination of optimized reaction conditions and the effect of the different molar ratio of Ni and Cu on the reaction rate of the oxidation reaction under the aerobic condition at room temperature.

Initially, the oxidation reactions of benzyl alcohol in the presence of H_2O catalyzed by 2.5 mol% of three Ni/Cu (1:1 **4a**/ 1:3 **4b**/ 3:1 **4c**) bimetallic NPs at room temperature about 10 min the maximum 55% yield of benzaldehyde for 56% conversion of benzyl alcohol was observed for catalyst Ni/Cu (3:1) **4c,** whereas minimum 35% yield with conversion 35% for Ni/Cu (1:1) **4a** (Table 2, entry 1). Unexpectedly, by expanding the reaction time up to 20 min or 30 min and catalyst loading 3.0 mol% or 3.5 mol%, the maximal 75% yield for 77% of conversion or 82% of benzaldehyde for 83% of conversion of benzyl alcohol was found for catalyst Ni/Cu (3:1) **4c,** respectively, while another two Ni/Cu (1:1) **4a** and for Ni/Cu (1:3) **4b** NPs gave less conversion with %yield (Table 2, entries 2, 3). However, optimized reaction conditions were detected with maximum 90% yield for 90% conversion, while the reaction was carried out catalyzed by 4.0 mol% of the Ni/Cu (3:1) **4c** bimetallic NPs at room temperature at 30 min (Table 2, entry 3). Moreover, no better yield was found by increasing the catalyst loading (5.0 mol%) and reaction time up to 40 min (Table 2, entry 5). Consequently, it was revealed from this optimization that the reaction rate and

Table 2 Optimized conditions of Ni/Cu **4a, 4b, and 4c** bimetallic NPs catalyzed oxidation of benzyl alcohol to benzaldehyde

Entry	Catalyst (mol%)	Time (min)	% Conv[a]	% Yield[a]	% Conv[b]	% Yield[b]	% Conv[c]	% Yield[c]
1	2.5	10	35	35	47	47	56	55
2	3.0	20	51	50	57	56	77	75
3	3.5	30	60	59	68	68	83	82
4	4.0	30	55	55	57	56	90	90
5	5.0	40	56	55	58	57	91	90

Reaction conditions: catalyst 4.0 mol%, alcohol (1.0 mmol), time 30 min, solvent H_2O (5 mL), room temperature (RT), and atmospheric air (O_2)

[a] Stands for % conversion of benzyl alcohol determined by GC and % yield of benzaldehyde for catalyst Ni/Cu (1:1) **4a**

[b] Stands for % conversion of benzyl alcohol determined by GC and % yield of benzaldehyde for catalyst Ni/Cu (1:3) **4b**

[c] Stands for % conversion of benzyl alcohol determined by GC and % yield of benzaldehyde for catalyst Ni/Cu (3:1) **4c**

% yield depend on the amount of Ni NPs more than the amount of Cu NPs of the Ni/Cu bimetallic NPs.

However, based on the observed optimized condition of the oxidation of benzyl alcohol catalyzed by Ni/Cu (3:1) **4c** bimetallic nanoparticles and for checking chemoselectivity of the oxidation for different types alcohols, we carried out this oxidation reaction of the broad scope of alcohols containing different sensitive functional group catalyzed by Ni/Cu (3:1) **4c** NPs' catalyst under above-optimized conditions and the results are listed in the following Tables 3 (entries 1–8).

Furthermore, although the reaction rate of the conversion of alcohol appeared to be slightly reduced with sterically constrained and electron-withdrawing groups and also a five-membered ring containing primary alcohols (Table 3, entries 1–8) in the case of a secondary alcohol, the full conversion was completed at 4 h under the same reaction conditions and the % yield cited in Table 4 (entries 1, 2).

However, Table 5 exhibits that this catalytic method is extremely chemoselective, because the oxidation reaction of a 1:1 mixture of a primary alcohol with secondary alcohol results in a quantitative conversion of the primary alcohol into an aldehyde after 30 min, while Ketone was produced only 5% of yield for 5% conversion of secondary alcohol (Entry 1).

Significantly, a far better result of chemoselectivity was observed when the oxidation of 1-(4-(hydroxymethyl)phenyl)ethanol **25** containing primary and secondary hydroxyl group on the same skeleton is carried out by this catalyst Ni/Cu (3:1) **4c** (Table 5, entry 2). After 30 min of the reaction, the only obtained product was 4-(1-hydroxyethyl)benzaldehyde without contamination of either the dicarbonyl compound or the isomeric keto alcohol.

All the carbonyl products were evaluated by ^{1}H, ^{13}C NMR (S4-S24 in the supplementary information), and also elemental analysis for solid products as well as compared with literature data.

Catalytic activity of Ni/Cu 4a, 4b, 4c bimetallic NPs for the chemoselective reduction of nitro groups of aromatic compounds

In recent years, bimetallic NPs catalyzed selective reduction of the aromatic nitro group at room temperature are also studied (Yang et al. 2017).

However, for studying the optimized conditions for the chemoselective reduction of the nitro group of aromatic substances into corresponding aniline derivatives catalyzed by the Ni/Cu bimetallic nanoparticle of different molar ratios (1:1 **4a**), (1:3 **4b**), and (3:1 **4c**), and also the effect of the different molar ratio of Ni and Cu on the reaction rate of the reaction, the reduction of the nitro group of 4-nitrophenol catalyzed by the synthesized Ni/Cu (1:1) **4a**, Ni/Cu (1:3) **4b**, and Ni/Cu (3:1) **4c** nanoparticles with hydrazine hydrate as a reducing agent under the aerobic conditions at room temperature was considered as the model reaction (Scheme 6).

Initially, in the absence of a catalyst or hydrazine hydrate in the presence of H_2O at room temperature under aerobic conditions, the advancement of the reactions was not observed (Table 6, entries 1, 2). Fascinatingly, by charging with 2.0 mol% of the three different bimetallic Ni/Cu **4a, 4b, 4c** NPs, when this reaction was continued individually in 10 min, the % yield of 4-aminophenol was attained as 40% for 41% conversion of 4-nitrophenol for catalyst Ni/Cu (1:1) **4a** and 50% yield for 51% conversion for Ni/Cu (1:3) **4b,** and also 60% yield for 60% conversion for Ni/Cu (3:1) **4c** at room temperature in water under aerobic conditions in the presence of hydrazine hydrate (Table 6, entry 3). Also, by adding the amount of NPs catalyst from 3.0 mol% to 3.5 mol% and increasing the reaction time up to 20 min, the maximum yield 89% for 89% conversion of 4-nitrophenol

Table 3 Oxidation of primary alcohols into the corresponding carbonyl compounds catalyzed by Ni/Cu (3:1) **4c** NPs' catalyst

Entry	Alcohol	Product	% Conv	% Yield
1	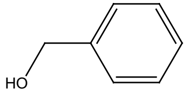 **5**	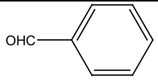 **13**	91	90
2	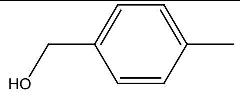 **6**	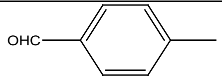 **14**	94	94
3	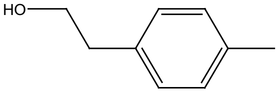 **7**	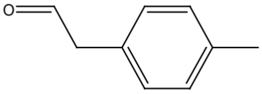 **15**	86	85
4	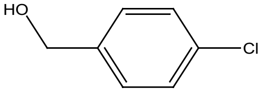 **8**	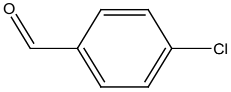 **16**	86	84
5	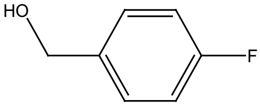 **9**	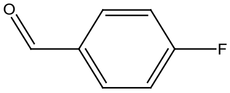 **17**	83	82
6	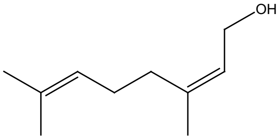 **10**	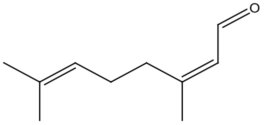 **18**	80	80
7	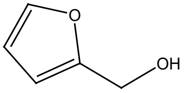 **11**	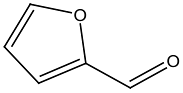 **19**	83	82
8	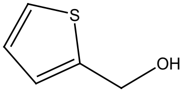 **12**	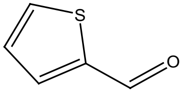 **20**	82	81

%Conversion of alcohols determined by GC and % yield calculated based on the respective alcohol. Reaction conditions: catalyst 4.0 mol%, alcohol (1.0 mmol), time 30 min, solvent H_2O (5 mL), room temperature (RT), and atmospheric air (O_2)

was isolated for catalyst Ni/Cu (3:1) **4c** (Table 6, entries 4, 5). However, the optimized condition was ascertained with maximal 96% yield for 97% conversion, while completing these reactions in 20 min with Ni/Cu nanoparticles (3:1) **4c** at room temperature in water under aerobic conditions using hydrazine hydrate as a reducing agent (Table 6, Entry 6). These outcomes indicate that Ni/Cu (3:1) **4c** is more active as a catalyst than Ni/Cu (1:1) **4a** and Ni/Cu (1:3) **4b**.

From this observation, owing to checking the chemoselectivity for the reduction of the nitro group in different aromatic compounds even in the presence of another reducible group catalyzed by the most active catalyst Ni/Cu (3:1) **4c** NPs' catalyst under the above-optimized conditions, this catalytic method was explored for a wide variety of substituted aromatic nitro-compounds for synthesizing the corresponding aromatic amines. The obtained results are included in Table 7. These results have shown that completely unchanged are the easily reducible functional groups such as CO, COMe, CO_2Me, COOH, F, N_3, and SCN, and accorded well to moderate % yield of products (Table 7, entries 2–10). The products were separated in a pure form directly by extraction with ethyl acetate.

All the amine products were analyzed by the ^1H and ^{13}C NMR spectrum (S25-S43 in the supplementary

Table 4 Oxidation of aromatic secondary alcohols into the corresponding carbonyl compounds catalyzed by catalyst Ni/Cu (3:1) **4c**

Entry	Alcohol	Product	% Conv	% Yield
1	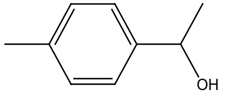 **21**	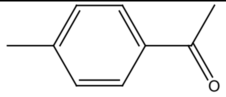 **23**	87	86
2	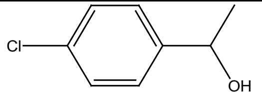 **22**	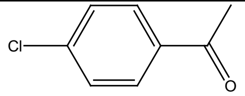 **24**	86	85

%Conversion of alcohols determined by GC and % yield calculated based on the respective alcohol. Reaction conditions: catalyst Ni/Cu (3:1)**4c** 4.0 mol%, alcohol (1.0 mmol), time 4 h, solvent H_2O (5 mL), and room temperature (RT)

Table 5 Chemoselective oxidation of alcohols catalyzed by Ni/Cu (3:1) **4c**

Entry	Alcohol	Product	% Conv	% Yield
1	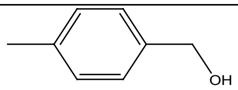 + 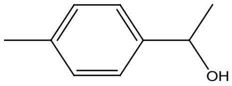	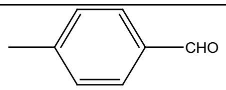 + 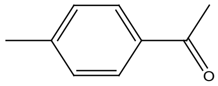	93 + 5	93 + 5
2	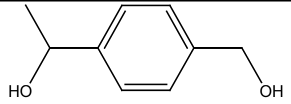 **25**	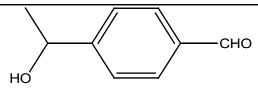 **26**	83	82

%Conversion determined by GC and % yield calculated based on the respective alcohol. Reaction conditions: catalyst 4.0 mol%, alcohol (1.0 mmol), time 30 min solvent H_2O (5 mL), room temperature (RT), and atmospheric air (O_2)

Table 6 Optimized conditions of Ni/Cu bimetallic NPs (1:1 **4a**), (1:3 **4b**), (3:1 **4c**) catalyzed reduction of 4-nitrophenol to 4-aminophenol

Entry	Catalyst (mol%)	NH_2-NH_2.H_2O	Time (min)	(%) Conv[a]	(%) Yield[a]	(%) Conv[b]	(%) Yield[a]	(%) Conv[c]	(%) Yield[c]
1	–	+	10	–	–	–	–	–	–
2	2.0	–	10	–	–	–	–	–	–
3	2.0	+	10	41	40	51	50	60	60
4	3.0	+	15	50	50	64	63	79	78
5	3.5	+	20	60	59	73	72	89	89
6	4.0	+	20	66	65	83	82	97	96

Reaction conditions: catalyst (4.0 mol%), solvent H_2O (5.0 mL), 4-nitrophenol (1.0 mmol), NH_2-NH_2.H_2O (0.5 mmol), time (20 min), room temperature (RT), and atmospheric air (O_2)

[a] Stands for % conversion of 4-nitrophenol determined by GC and % yield of 4-aminophenol for catalyst Ni/Cu (1:1) **4a**, similarly

[b] Stands for % conversion of 4-nitrophenol determined by GC and % yield of 4-aminophenol for catalyst Ni/Cu (1:3) **4b**

[c] Stands for % conversion of 4-nitrophenol determined by GC and % yield of 4-aminophenol for catalyst Ni/Cu (3:1) **4c**

Table 7 Reduction of substituted nitro benzenes to the corresponding anilines catalyzed by Ni/Cu (3:1) **4c**

Serial no.	Substrate	Product	(%) Conv	(%) Yield
1	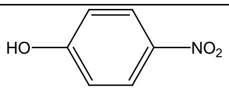 **27**	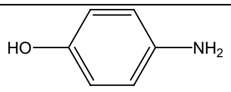 **37**	96	96
2	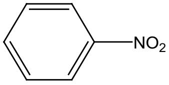 **28**	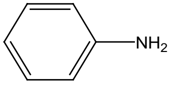 **38**	89	88
3	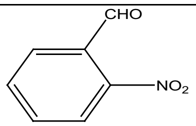 **29**	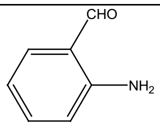 **39**	97	97
4	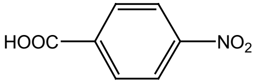 **30**	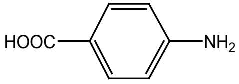 **40**	92	91
5	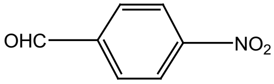 **31**	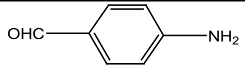 **41**	96	96
6	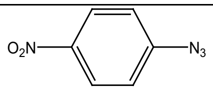 **32**	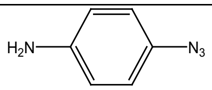 **42**	94	93
7	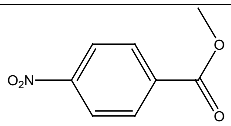 **33**	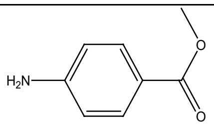 **43**	92	91
8	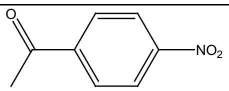 **34**	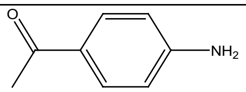 **44**	94	93
9	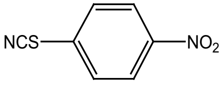 **35**	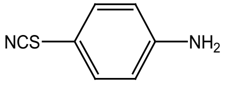 **45**	95	95
10	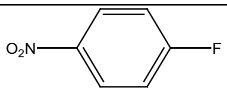 **36**	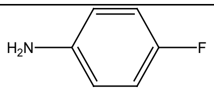 **46**	88	87

%Conversion determined by GC and % yield calculated based on their respective nitro compound. Reaction conditions: catalyst Ni/Cu (3:1)**4c**, (4.0 mol%), solvent H_2O (5.0 mL), substituted nitro compounds (1.0 mmol), NH_2-NH_2.H_2O (0.5 mmol), time (20 min), and atmospheric air (O_2)

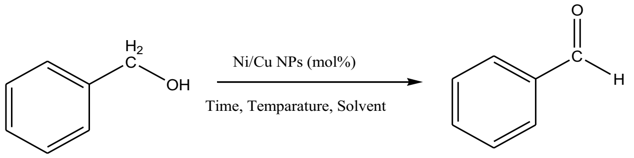

Scheme 5 Optimization of Ni/Cu **4a, 4b, and 4c** bimetallic NPs catalyzed oxidation of benzyl alcohol to benzaldehyde

Table 8 % Yield of benzaldehyde for different catalytic run by Ni/Cu (3:1) **4c** NPs

Run	Yield (%)
1	85
2	84
3	84
4	83
5	80

information) and also elemental analysis for solid products in addition to associated with the literature data.

Heterogeneity test of the catalyst Ni/Cu (3:1) 4c

Initially, a mixture of Ni/Cu (3:1) **4c** NPs (4.0 mol%) and benzyl alcohol (1.0 mmol) in water (5 mL) was stirred for 15 min at room temperature. Then, the reaction was stopped and centrifuged of the reaction mixture and also filtered off the catalyst. By analyzing the solution with ^{1}H NMR, 50% conversion of benzyl alcohol into benzaldehyde was found and the experiment further proceeded for another 15 min with that filtrate solution. The concentration of the benzaldehyde was not increased, as calculated by the study of ^{1}H NMR. Moreover, the leaching study of metal of heterogeneous catalyst is very significant, and for this, Ni and Cu leaching analysis after separating off the catalyst was done using ICP-OES and no leaching of Ni and Cu was observed.

Recoverability and reusability of the catalyst Ni/Cu (3:1) 4c

The recoverability and reusability of the catalyst **4c** were tested considering the reaction of oxidation of benzyl alcohol to benzaldehyde (Scheme 5), and the % yield of benzaldehyde is cited in Table 8. The catalyst was recovered by centrifugation after each catalytic run followed by ethanol and acetone washing (2 × 3 mL) and also reused to further catalytic run. After recycling five times, the results of XRD and SEM analysis showed the necessary peaks for the recovered catalyst's FCC structure of the catalyst (Fig. 12) and agglomerated spherical surface morphology (Fig. 11) distinctly. The specific peak intensity of the recycled catalyst was reduced, suggesting that the structure of the recycled Ni/Cu (3:1) **4c** was slightly demolished during the oxidation of benzyl alcohol under present reaction conditions (Fig. 12). However, these detected results suggest that the catalyst is not only actively satisfactory for the reaction but also very stable (Scheme 6).

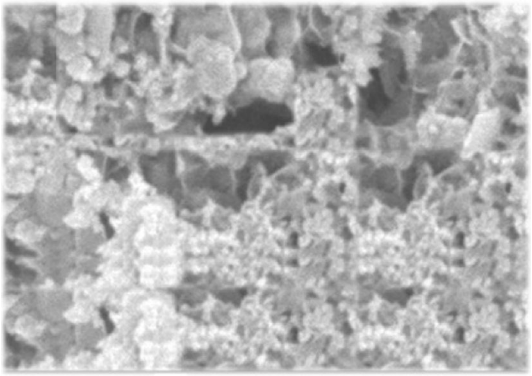

Fig. 11 SEM of the recovered catalyst Ni/Cu (3:1) **4c**

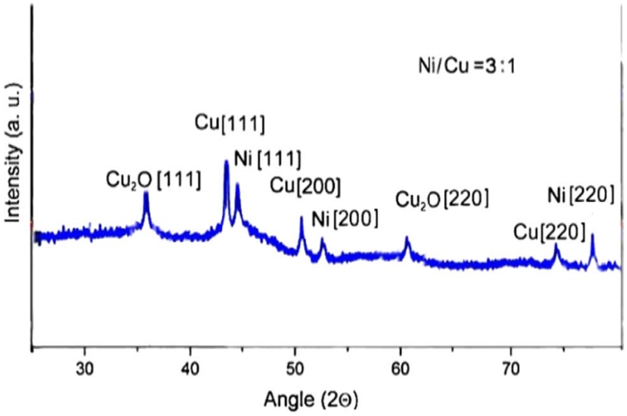

Fig. 12 XRD of the recovered catalyst Ni/Cu (3:1) **4c**

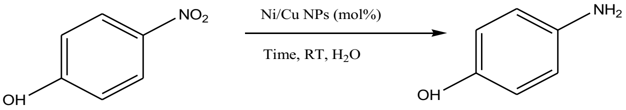

Scheme 6 Optimization of Ni/Cu bimetallic nanoparticles **4a, 4b,** and **4c** catalyzed reduction of 4-nitrophenol to 4-aminophenol

Reaction conditions: Ni/Cu (3:1) **4c** NPs (4.0 mol%), benzyl alcohol (1.0 mmol) in water (5 mL), room temperature, and time 30 min.

Conclusions

In summary, Ni/Cu bimetallic nanoparticles with molar ratios (1:1) **4a**, (1:3) **4b**, (3:1) **4c** supported by dendritic ligand 2,4,6-Tris (di-4-chlorobenzamido)-1,3-diazine **3** were prepared. Among the different molar ratios of Ni and Cu (1:1 **4a** or 1:3 **4b**), the catalyst Ni/Cu (3:1) **4c** has shown excellent activity for the rapid chemoselective oxidation of primary alcohols to aldehydes at 30 min and reduction of the nitro substrates in the vicinity of other easily reducible functional groups to the corresponding anilines at 20 min in an aqueous medium with a high degree of chemoselectivity under very mild conditions. Also, this heterogeneous Ni/Cu bimetallic nanocatalyst is easily recoverable and reusable at least five times without any significant loss of activity. However, selective oxidation and reduction of biologically active organic compounds in an aqueous medium at room temperature and various carbon–carbon cross-coupling reactions such as Heck, Suzuki, Stille carbon–carbon cross-coupling reactions can be studied by this green catalytic approach.

Acknowledgements The authors would like to express their innermost gratitude to the Ministry of Science and Technology, Government of the People's Republic of Bangladesh, Dhaka, Bangladesh (National Science and Technology, Grant No.:39.00.0000.012.002.04.19-08 (2019-2020) and Bangladesh University of Engineering and Technology (BUET), Dhaka, Bangladesh for providing financial support to perform this research work.

Compliance with ethical standards

Conflict of interest The authors have no conflicts of interest.

References

Addis D, Shaikh N, Zhou S (2010) Chemo- and stereoselective iron-catalyzed hydrosilylation of ketones. Chem Asian J 5:1687–1691

Alhumaimess M, Lin Z, Weng W (2012) Oxidation of benzyl alcohol by using gold nanoparticles supported on ceria foam. Chemsuschem 5:125–131

Alshammari H, Alhumaimess M, Alotaibi MH, Alshammari AS (2017) Catalytic activity of bimetallic AuPd alloys supported MgO and MnO_2 nanostructures and their role in selective aerobic oxidation of alcohols. J King Saud Univ Sci 29:561–566

An K, Somorjai GA (2015) Nanocatalysis I: synthesis of metal and bimetallic nanoparticles and porous oxides and their catalytic reaction studies. Catal Lett 145:233–248

Balcha T, Strobl JR, Fowler C (2011) Selective aerobic oxidation of crotyl alcohol using AuPd core-shell nanoparticles. ACS Catal 1:425–436

Chalker JM, Wood CSC, Davis BG (2009) A convenient catalyst for aqueous and protein Suzuki−Miyaura cross-coupling. J Am Chem Soc 131:16346–16347

Chatterjee A, Ward TR (2016) Recent advances in the palladium catalyzed suzuki-miyaura cross-coupling reaction in water. Catal Lett 146:820–840

Currall K, David SJ (2014) Hydrogenation of 4-nitroacetophenone over Rh/Silica: understanding selective hydrogenation of multifunctional molecules. Top Catal 57:1519–1525

Dimitratos N, Lopez-Sanchez AJ, Hutchings JG (2012) Selective liquid phase oxidation with supported metal nanoparticles. Chem Sci 3:20–44

Gong X, Liu B, Zhang G (2016) A mild and environmentally benign strategy towards hierarchical CeO_2/Au nanoparticle assemblies with crystal facet-enhanced catalytic effects for benzyl alcohol aerobic oxidation. CrystEngComm 18:5110–5120

Harada T, Ikeda S, Hashimoto F (2010) Catalytic activity and regeneration property of a Pd nanoparticle encapsulated in a hollow porous carbon sphere for aerobic alcohol oxidation. Langmuir 26:17720–17725

Harraz FA, El-Hout SE, Killa HM, Ibrahim IA (2012) Palladium nanoparticles stabilized by polyethylene glycol: Efficient, recyclable catalyst for hydrogenation of styrene and nitrobenzene. J Catal 286:184–192

Hosseini-Sarvari M, Razmi Z (2015) Direct hydrogenation and one-pot reductive amidation of nitro compounds over Pd/ZnO nanoparticles as a recyclable and heterogeneous catalyst. Appl Surf Sci 324:265–274

Ishikawa N (1994) The fluorochemical industry. In: Banks RE, Smart BE, Tatlow JC (eds) Organofluorine chemistry: principles and commercial applications. Springer, Boston, pp 609–615

Islam MS, Khan MW (2019) Synthesis of triazine-based dendrimer assisted Pd-Cu bimetallic nanoparticles and catalytic activity for C-C coupling reactions. Nanosci Nanotechnol 9:1–21

Islam S, Khan W (2020) Synthesis and comparative study of catalytic activity between Pd-metallodendrimer and Pd/Cu-bimetallodendrimer nanoparticle-based on triazine. J Saudi Chem Soc 24:105–119

Jiang X, Ma S (2018) Studies on iron-catalyzed aerobic oxidation of benzylic alcohols to carboxylic acids. Synthesis 50:1629–1639

Kimi M, Jaidie MMH, Pang SC (2018) Bimetallic Cu-Ni nanoparticles supported on activated carbon for catalytic oxidation of benzyl alcohol. J Phys Chem Solids 112:50–53

Lee W, Piao L, Park C-H et al (2010) Facile synthesis and size control of spherical aggregates composed of Cu_2O nanoparticles. J Colloid Interface Sci 342:198–201

Liu L, Lou H, Chen M (2016) Selective hydrogenation of furfural to tetrahydrofurfuryl alcohol over Ni/CNTs and bimetallic CuNi/CNTs catalysts. Int J Hydrog Energy 41:14721–14731

Liu L, Zhou X, Yan Y (2018) Bimetallic gold-silver nanoparticles supported on zeolitic imidazolate framework-8 as highly active heterogenous catalysts for selective oxidation of benzyl alcohol into benzaldehyde. Polymers 10:1089

Mondal P, Purkait MK (2017) Green synthesized iron nanoparticle-embedded pH-responsive PVDF-co-HFP membranes: optimization study for NPs preparation and nitrobenzene reduction. Sep Sci Technol 52:2338–2355

Pagoti S, Surana S, Chauhan A (2013) Reduction of organic azides to amines using reusable Fe_3O_4 nanoparticles in aqueous medium. Catal Sci Technol 3:584–588

Pan S, Yan S, Osako T, Uozumi Y (2018) Controlled aerobic oxidation of primary benzylic alcohols to aldehydes catalyzed by polymer-supported triazine-based dendrimer-copper composites. Synlett 29:1152–1156

Pritchard J, Kesavan L, Piccinini M (2010) Direct synthesis of hydrogen peroxide and benzyl alcohol oxidation using Au−Pd catalysts prepared by sol immobilization. Langmuir 26:16568–16577

Reddy CR, Reddy SR, Naidu S (2015) Chemoselective oxidation of benzyl, amino, and propargyl alcohols to aldehydes and ketones under mild reaction conditions. ChemistryOpen 4:107–110

Rezaei SJT, Malekzadeh AM, Poulaei S (2018) Chemo-selective reduction of nitro and nitrile compounds using Ni nanoparticles immobilized on hyperbranched polymer-functionalized magnetic nanoparticles. Appl Organomet Chem 32:e3975

Shao M-H, Sasaki K, Adzic RR (2006) Pd−Fe nanoparticles as electrocatalysts for oxygen reduction. J Am Chem Soc 128:3526–3527

Sharif MdJ, Yamazoe S, Tsukuda T (2014) Selective hydrogenation of 4-nitrobenzaldehyde to 4-aminobenzaldehyde by colloidal RhCu bimetallic nanoparticles. Top Catal 57:1049–1053

Sharma G, Kumar A, Sharma S (2019) Novel development of nanoparticles to bimetallic nanoparticles and their composites: a review. J King Saud Univ Sci 31:257–269

Sun J, Han Y, Fu H (2017) Au@Pd/TiO_2 with atomically dispersed Pd as highly active catalyst for solvent-free aerobic oxidation of benzyl alcohol. Chem Eng J 313:1–9

Takasaki M, Motoyama Y, Higashi K (2008) Chemoselective hydrogenation of nitroarenes with carbon nanofiber-supported platinum and palladium nanoparticles. Org Lett 10:1601–1604

Vollhardt D, Liu F, Rudert R (2005) Molecular recognition of dissolved pyrimidine derivatives by a dialkyl melamine-type monolayer. ChemPhysChem 6:1246–1250

Wu Y, Cai S, Wang D (2012) Syntheses of water-soluble octahedral, truncated octahedral, and cubic Pt–Ni nanocrystals and their structure-activity study in model hydrogenation reactions. J Am Chem Soc 134:8975–8981

Yagai S, Kitamoto Y, Datta S, Adhikari B (2019) Supramolecular polymers capable of controlling their topology. Acc Chem Res 52:1325–1335

Yang S, Yue W, Huang D (2012a) A facile green strategy for rapid reduction of graphene oxide by metallic zinc. RSC Adv 2:8827–8832

Yang X, Yang Q, Xu J, Lee C-S (2012b) Erratum: bimetallic PtPd nanoparticles on Nafion-graphene film as catalyst for ethanol electro-oxidation. J Mater Chem 22:8057–8062

Yang C, Xue W, Yin H (2017) Hydrogenation of 3-nitro-4-methoxy-acetylaniline with H_2 to 3-amino-4-methoxy-acetylaniline catalyzed by bimetallic copper/nickel nanoparticles. New J Chem 41:3358–3366

Zhang J, Lu G, Cai C (2016) Chemoselective transfer hydrogenation of nitroarenes by highly dispersed Ni-Co BMNPs. Catal Commun 84:25–29

Zimmerman SC, Lawless LJ (2001) Supramolecular chemistry of dendrimers. In: Vögtle F, Schalley CA (eds) Dendrimers IV: metal coordination, self assembly, catalysis. Springer, Berlin, pp 95–120